Available online at www.sciencedirect.com

ScienceDirect

IFAC Papers Online CONFERENCE PAPER ARCHIVE

IFAC PapersOnLine 50-1 (2017) 15847–15852

A Cybernetic Analysis of Maximum Unnoticeable Added Dynamics for Different Baseline Controlled Systems

I. Matamoros, * **T. Lu,** * **M.M. van Paassen** * **and D.M. Pool** *

* *Control and Simulation Section, Aerospace Engineering, Delft University of Technology, 2629 HS, Delft, The Netherlands (e-mail: i.matamoroscid@student.tudelft.nl, {t.lu-3, m.m.vanpaassen, d.m.pool}@tudelft.nl).*

Abstract: Maximum unnoticeable added dynamics (MUAD) envelopes have been largely used to assess the adequacy of low-order equivalent systems (LOES) in handling qualities assessment and simulator validation. However, research has shown that more thorough verification of the adequacy of this method is required. This paper studies the influence of the baseline aircraft dynamics on the MUAD envelopes. The assessment is based on quantitative measures of pilot control behaviour obtained with the cybernetic approach. The measures were taken from a human-in-the-loop pitch tracking task experiment with compensatory display. The results are consistent with the MUAD envelopes and reveal no interaction effects of the baseline and added dynamics on the pilot control behaviour. This suggests that, under the considered conditions, the MUAD envelopes shall remain constant independently of the bandwidth of the baseline controlled dynamics.

Keywords: Manual control, Vehicle dynamics, Human factors, Human control modeling, Handling qualities

1. INTRODUCTION

In aircraft handling qualities research, the true nonlinear and often high-order (i.e., due to control augmentation) dynamics of aircraft (Neal and Smith, 1971) are typically approximated with their low-order equivalent systems (LOES) (Hodgkinson, 2005). LOES are low-order simplifications of true high-order aircraft dynamics that aim to capture their fundamental dynamic modes while reducing the system to a more tractable low-order form. Although such LOES simplify the analysis and control augmentation development, the adequacy of the level of mismatch between the true dynamics and its LOES is of particular relevance. For handling qualities, the validity of a LOES is directly dependent on human sensitivity to subtle differences in the controlled vehicle dynamics (Wood and Hodgkinson, 1980).

To investigate this sensitivity, the acceptable levels of mismatch between a system and its LOES were first analyzed in the early 1980s by Wood and Hodgkinson (1980). This research resulted in the definition of envelopes for the Maximum Unnoticeable Added Dynamics (MUAD), based on subjective pilot ratings of noticeability. The derived envelopes define frequency-dependent limits that encompass the maximum levels of mismatch that are imperceptible to human pilots (Wood and Hodgkinson, 1980; MIL, 2004). Consistent with knowledge of human manual control (McRuer and Jex, 1967), MUAD envelopes are narrow in the frequency range critical to manual control performance, and notably wider at low and high frequencies. Recently, it has been stressed by Mitchell et al. (2006) that such envelopes depend on the dynamic characteristics – i.e., bandwidth – of the baseline (reference) vehicle dynamics, a dependency that would greatly complicate the task of defining universal envelopes for allowable levels of mismatch. Still, given their straightforward applicability and their intuitive soundness, the MUAD envelopes have become a *de facto* standard to assess the adequacy of LOES (Field et al., 2003; Bosworth and Williams-Hayes, 2007; Geluardi et al., 2014).

MUAD envelopes are traditionally determined from extensive human-in-the-loop experiments, where subjective ratings are used to determine the noticeability of added dynamics (Wood and Hodgkinson, 1980; Mitchell et al., 2006). The main drawback of subjective assessment methods is their poor reproducibility. A potentially valuable alternative, given the known adaptability of human control dynamics to changes in the controlled system (McRuer and Jex, 1967), is to use a *cybernetic approach* (Mulder et al., 2013; Pool and Zaal, 2016). The cybernetic approach enables objective detection of changes in pilot control by fitting control-theoretic models of human behavior with physically interpretable parameters to experimental data. This approach has been used to quantify the sensitivity of human control behavior to many different factors such as simulator fidelity assessment (Zaal et al., 2009b; Mulder et al., 2013; Pool and Zaal, 2016), but not yet for investigating MUAD.

In this paper, maximum unnoticeable added dynamics and their dependence on the dynamics of the baseline (BSL) controlled system are determined using an objective

10.1016/j.ifacol.2017.08.2328

cybernetic approach, which has been applied successfully in previous research on manual control (Mulder et al., 2013; Pool and Zaal, 2016). A human-in-the-loop simulator experiment is described with which human pitch tracking data was collected for added dipole dynamics of increasing magnitude perturbing the baseline controlled dynamics (Wood and Hodgkinson, 1980). To tie in with (Mitchell et al., 2006), this was done for two baseline LOES dynamics, representative for low-bandwidth (i.e., sluggish) and high-bandwidth (i.e., responsive) aircraft. From this data, the individual and combined effects of the variation in baseline and added dynamics on human pilots' control behavior were determined, to verify any effects of the baseline dynamics on the MUAD.

This paper is structured as follows. In Section 2 the experimental setup, procedures and methodologies are presented. The obtained results are given in Section 3 and discussed in Section 4. Conclusions are drawn in Section 5.

2. EXPERIMENT

2.1 Pitch Attitude Control Task

Participants were asked to perform a pitch tracking task with compensatory display, equivalent earlier experiments (Zaal et al., 2009b; Pool and Zaal, 2016). A block diagram of the task is given in Fig. 1.

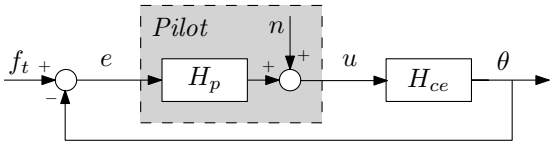

Fig. 1. Compensatory pitch tracking task.

In this task the pilot's goal is to minimize the tracking error e between the controlled system's pitch attitude θ and the target signal f_t. In the compensatory task of Fig. 1, the pilot only receives feedback of the tracking error e and provides a single control input u. Hence, human control behavior in this task is described by the single linear response function H_p. The non-causal pilot behavior not captured by H_p is represented by the remnant signal n.

In Fig. 1, the controlled dynamics are given by H_{ce}, which in our experiment was defined as the cascaded transfer function of the baseline dynamics H_{base} and certain added dynamics H_{add}:

$$H_{ce}(s) = H_{\text{base}}(s)H_{\text{add}}(s) \tag{1}$$

2.2 Apparatus

The experiment was performed in the fixed-base simulator setup of the Human-Machine Interaction Laboratory at TU Delft, see Fig. 2. The participants sat at the right seat and gave pitch control input commands through an hydraulic side stick with a maximum ±22° excursion in pitch. The roll axis of the stick was locked at 0° to ensure pure pitch commands. The tracking error was shown to the pilot on the primary heads-down display, which showed a simplified artificial horizon display where e was shown as the vertical distance between the aircraft symbol and the horizon line, see Fig. 3.

Fig. 2. Experiment setup.

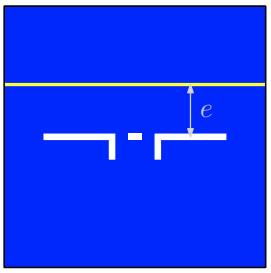

Fig. 3. Visual display.

2.3 Baseline Dynamics

The baseline dynamics H_{base} were a simplified second-order LOES of aircraft pitch dynamics, as for instance also considered by Mitchell et al. (2006):

$$H_{\text{base}}(s) = M_{\delta_e}\frac{M_q}{s(s+M_q)} \tag{2}$$

In Eq. (2), M_q and M_{δ_e} are the pitch damping and elevator control effectiveness coefficients, respectively. Two baseline dynamics were considered in the experiment, see Table 1. The dynamics differed in terms of M_q, for which values resembling those tested by Mitchell et al. (2006) were chosen to achieve two baseline dynamics with low bandwidth (LBW, M_q=1.5 rad/s) and high bandwidth (HWB, M_q=3 rad/s). These dynamics are representative of sluggish (big) aircraft, and fast-responding (small) aircraft, respectively. The frequency responses of both tested baseline dynamics are shown in Fig. 4.

Table 1. Baseline dynamics configurations.

Baseline dynamics	M_q (rad/s)	M_{δ_e} (-)
LBW	1.5	-1.5
HBW	3.0	-1.5

2.4 Added Dynamics

To be able to intuitively vary the magnitude of the perturbation of H_{ce}, the added dynamics in the experiment were chosen as positive-magnitude dipoles, also previously used in Carpenter and Hodgkinson (1980), given by:

$$H_{\text{add}}(s) = \frac{s^2 + 2\omega_{dp}\zeta_z s + \omega_{dp}^2}{s^2 + 2\omega_{dp}\zeta_p s + \omega_{dp}^2} \tag{3}$$

The dipole central frequency ω_{dp} was set to 3 rad/s, which is in the range of predominant frequencies of manual control (McRuer and Jex, 1967) and, consequently, in the region where MUADs are the most narrow (Wood and Hodgkinson, 1980). The denominator damping ratio ζ_p was fixed at 0.2, while the numerator damping ratio ζ_z was an independent variable varied from 0.2 to 0.7. The seven considered added dynamics configurations are shown in Fig. 5, together with the MUAD envelope from Wood and Hodgkinson (1980) shown in gray. Note that for the baseline (BSL) condition $\zeta_z = \zeta_p = 0.2$ and thus $H_{\text{add}} = 1$. Note from Fig. 5 that for $\zeta_z \geq 0.5$ H_{add} is outside of the MUAD in both magnitude and phase.

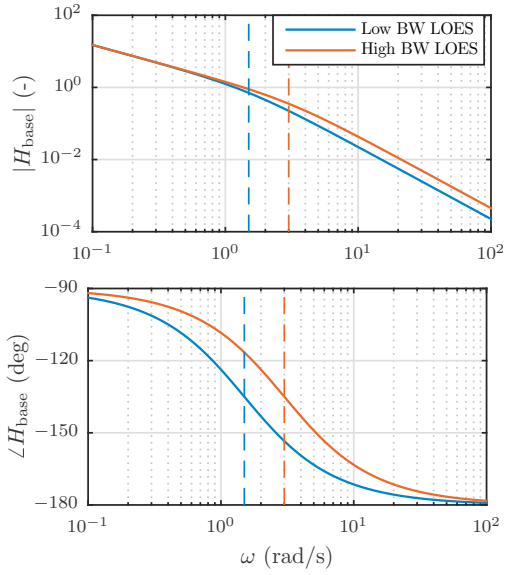

Fig. 4. Baseline dynamics frequency responses. Vertical dashed lines indicate M_q values.

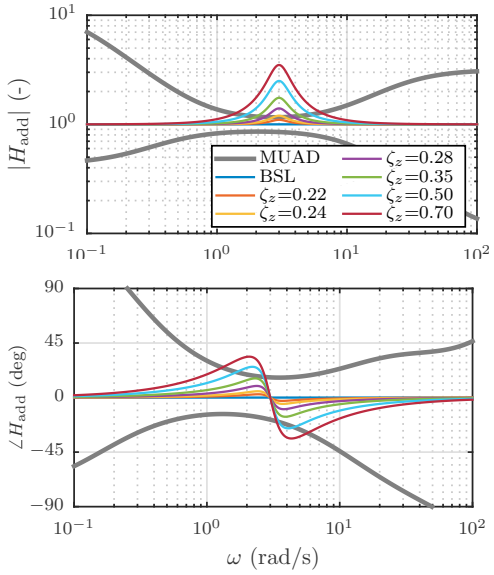

Fig. 5. Added dynamics frequency responses. Gray lines indicate MUAD from (Wood and Hodgkinson, 1980).

2.5 Pilot Model

It is well-known that in manual control, human pilots adapt their own control dynamics H_p to those of the controlled element H_{ce} to ensure adequate closed-loop system characteristics and tracking performance (McRuer and Jex, 1967). For the baseline dynamics considered in our experiment (see Eq. (2)), pilots are required to generate lead equalization to counter the controlled element lag due to M_q. Hence, the accepted model for H_p is:

$$H_p(s) = K_p(T_L s + 1)e^{-s\tau_p} H_{\text{nm}}(s) \tag{4}$$

$$H_{\text{nm}}(s) = \frac{\omega_{\text{nm}}^2}{\omega_{\text{nm}}^2 + 2\zeta_{\text{nm}}\omega_{\text{nm}} s + s^2} \tag{5}$$

In Eq. (4), K_p is the pilot control gain and T_L is the lead time-constant. The delay term τ_p accounts for the time delay in the pilot's response. Finally, the neuromuscular dynamics are modeled as a second-order mass-spring-damper system, where the damping ratio ζ_{nm} and natural frequency ω_{nm} are parameters to be estimated. Overall, the five parameters of the model of Eq. (4) can be used to quantify changes in pilot control dynamics.

2.6 Forcing Functions

The target signal f_t, see Fig. 1, was defined as a sum of 10 sines with different frequencies, amplitudes and phase shifts, as used in (Zaal et al., 2009b):

$$f_t(t) = \sum_{k=1}^{10} \left(A_t(k)\sin(\omega_t(k)t + \phi_t(k))\right) \tag{6}$$

To facilitate estimating a frequency response function (FRF) of H_p using spectral methods (van Paassen and Mulder, 1998), the frequencies ω_t are integer multiples (n_t) of the experimental measurement time base frequency $\omega_m = 2\pi/T_m$, with $T_m = 81.92$ s as the total measurement time. The integer factors n_t have the same values as in (Zaal et al., 2009b), and are listed in Table 2 along with the frequencies, amplitudes and phase shifts. The target signal was defined to have a variance of 1.6 deg^2.

Table 2. Forcing function parameters.

k	n_t	ω_t (rad/s)	A_t (deg)	ϕ_t (rad)
1	6	0.460	1.397	1.288
2	13	0.997	0.977	6.089
3	27	2.071	0.441	5.507
4	41	3.145	0.237	1.734
5	53	4.065	0.159	2.019
6	73	5.599	0.099	0.441
7	103	7.900	0.063	5.175
8	139	10.661	0.046	3.415
9	194	14.880	0.036	1.066
10	229	17.564	0.033	3.479

2.7 Participants and Experiment Procedures

Seven participants volunteered to perform the experiment and provided written informed consent before their participation. All had previous experience with manual control tasks equivalent to the one performed in the experiment. Each participant performed 14 experimental conditions: the factorial combination of the two baseline dynamics (HBW and LBW) and seven added dynamics (see Fig. 5).

Participants were instructed to minimize the tracking error shown on the compensatory display throughout the experiment. The experiment was performed in two sessions, one for each baseline dynamics setting. At the start of each session, participants performed four training runs with no added dynamics, to familiarize themselves with the baseline dynamics. Subsequently, the seven added dynamics settings were tested, in a balanced randomized order defined by a Latin square. The order testing for the HBW and LBW baseline dynamics was balanced, i.e., four of the participants tested the HBW case first, while the other three controlled the LBW system in the first session. This was done to minimize the effects continued training and fatigue on the comparison of conditions.

For each condition, a total of four repeated runs were performed, followed by a single tracking run with the

baseline dynamics only. For each run, the time histories of all control loop signals – i.e., e, u, and θ – were recorded.

2.8 Dependent variables

Changes in participants' control behavior over the different experiment conditions were quantified using two different sets of dependent variables:

- *Tracking performance and control effort.* For each condition, tracking performance and control effort were measured as the root mean square (RMS) of the tracking error (e) and control (u) signals, respectively.
- *Pilot model parameters.* Estimated values of K_p, T_L, τ_p, ω_{nm} and ζ_{nm} were used to quantify participants' changes in control dynamics. These parameters were estimated using the time-domain pilot model fitting technique of (Zaal et al., 2009a).

All dependent variables were calculated for the last three tracking runs performed for each condition and then averaged. The first run of each condition was discarded to eliminate the effect of time-varying pilot responses due to adaptation to the new controlled dynamics. These final results were analyzed with a two-way repeated-measures ANOVA for statistically significant effects of the bandwidth (BW) of the baseline dynamics and the added dynamics (AD) over all conditions.

3. RESULTS

3.1 Tracking Performance and Control Effort

Fig. 6 shows the RMS of the tracking error e and the control signal u, averaged over the last three runs of each experimental condition and over the seven subjects. Data for the low-BW and high-BW baseline dynamics are shown in blue and red, respectively. Error bars indicate standard deviations. To facilitate comparison with the baseline condition, the shaded areas indicate the 95% confidence intervals for both baseline conditions where $H_{\text{add}} = 1$. The statistical analysis results for the data shown in Fig. 6 are listed in Table 3.

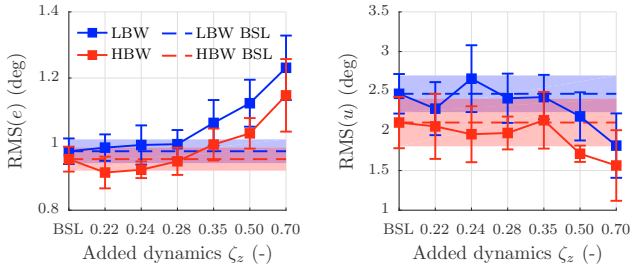

(a) Tracking performance. (b) Control effort.

Fig. 6. Average error and control RMS, with LBW and HBW baseline data in blue and red, respectively.

Fig. 6(a) shows that the task was easier for the HBW dynamics, as these controlled dynamics – with increased gain and reduced phase lag compared to the LBW setting – were more responsive. Error RMS values were significantly lower for the high-BW dynamics (red data) than for the LBW dynamics, see Table 3, BW. Furthermore, a clear increase in RMS(e) with increasing dipole damping ratio ζ_z is observed in Fig. 6(a). This effect was expected, as with higher ζ_z, the perturbation of the controlled dynamics by the added dipole is larger. This effect of the added dynamics on the error RMS is highly significant, see Table 3, BW.

Table 3. ANOVA results for RMS data.

Independent variables		Dependent variables			
		RMS(e)		RMS(u)	
Factor	df	F	Sig.	F	Sig.
BW	1	13.7	*	6.3	*
AD	6	34.1	**	11.9	**
BW × AD	6	0.5	-	1.0	-

Note: ** is highly significant ($p < 0.01$), * is significant ($0.01 \leq p < 0.05$), and − is not significant ($p \leq 0.05$).

Fig. 6(b) and Table 3 show that control effort is significantly lower for the high-BW dynamics, as expected given their overall higher gain, see Fig. 4. Increased ζ_z is further seen to result in reduced control effort (lower RMS(u)), a highly significant effect (see Table 3, AD).

Finally, the effects of ζ_z on task performance and control effort are found to be equivalent for the low and high-BW baseline dynamics. For both, the data for added dynamics with $\zeta_z = 0.35 - 0.5$ are the first to be outside of the 95% confidence intervals for their respective baseline measurements. The two-way ANOVAs performed on these dependent variables also show no significant interaction effects (BW × AD), see Table 3. Therefore, Fig. 6 shows no evidence for a strong dependence of the noticeability of added dynamics on the baseline controlled element.

3.2 Pilot Identification Results

Fig. 7 shows a representative example pilot identification result, with the H_p FRF estimate at ω_t indicated with black asterisks and the fitted H_p model of Eq. (4) with a red line. Furthermore, the frequency responses of the controlled element H_{ce} and the open-loop dynamics $H_{ol} = H_p H_{ce}$ are plotted with gray and blue lines, respectively.

Fig. 7 shows very good agreement between the FRF and estimated model for the pilot control dynamics. Furthermore, the Variance Accounted For of the fitted model is 73.5%, meaning that the model explains 73.5% of the measured control signal u. For all fitted tracking run data, equivalent results and VAFs of over 70% were obtained, which is the expected accuracy with which single-run human control data may be explained by an H_p model (Zaal et al., 2009a). As is clear from the H_p data in Fig. 7, participants did not explicitly compensate for the added dipole dynamics evident at 3 rad/s in both the frequency responses of H_{ce} and H_{ol}. Therefore, these results confirm the selection of the appropriate model structure for H_p.

Fig. 8 shows the estimated pilot model parameters averaged over the seven participants. Error bars indicate standard deviations. Again, blue and red markers indicate data for the LBW and HBW conditions and the shaded areas show the 95% confidence intervals for their respective baseline conditions. Table 4 presents the corresponding statistical analysis results.

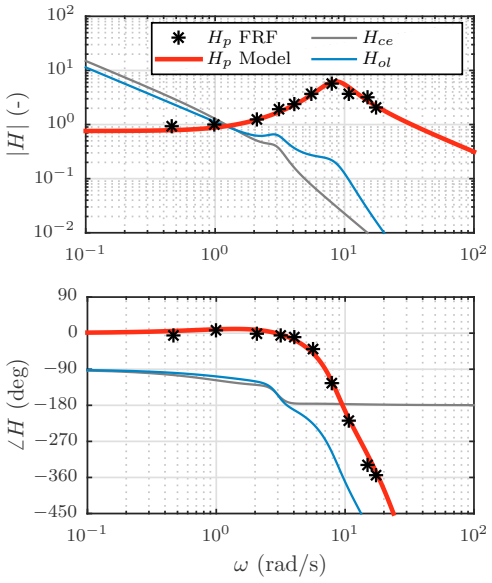

Fig. 7. Example pilot identification data for subject 7, LBW baseline dynamics, $\zeta_z = 0.35$, run 2.

Table 4. ANOVA results for pilot parameters.

Independent variables		Dependent variables					
		K_v		T_L		τ_v	
Factor	df	F	Sig.	F	Sig.	F	Sig.
BW	1	0.2	-	27.5	**	1.2	-
AD	6	33.2	**	2.4	-	8.1	**
BW × AD	6	1.2	-	1.3	-	0.7	-

Note: ** is highly significant ($p < 0.01$), * is significant ($0.01 \leq p < 0.05$), and − is not significant ($p \leq 0.05$).

Matching the degraded task performance and decreasing control effort with increasing ζ_z, Fig. 8(a) shows a significant decrease in K_p, see Table 4, that is equivalent for both tested baseline dynamics. For $\zeta_z = 0.7$, K_p reduces to less than 50% of its value for the baseline conditions. Fig. 8(c) shows that also the pilot delay τ_p is significantly affected by the added dipole dynamics, as it decreases by around 50 ms for $\zeta_z = 0.7$ compared to the baseline data. This suggests that due to the presence of the dipole resonance peak, participants responded quicker to tracking errors, implying increased workload (McRuer and Jex, 1967).

Fig. 8 and Table 4 further show that T_L, ω_{nm} and ζ_{nm} are not notably affected by the different added dynamics settings. The lead time-constant T_L, see Fig. 8(b), is found to be significantly different for both baseline controlled elements, see Table 4. As lead equalization is needed to compensate for the controlled element lag at M_q (McRuer and Jex, 1967), it is expected that $T_L \approx 1/M_q$. The average lead time constants of 0.53 s and 0.38 s for the LBW and HBW baseline dynamics, respectively, are very close to these expected values. The fact that no variation in T_L with ζ_z is found is somewhat surprising, given the additional lead and lag generated by the dipoles around $\omega_{dp} = 3$ rad/s, which is close to the tested M_q settings.

Finally, as can be verified from Table 4 and Fig. 8, the estimated pilot parameters show no evidence for a significant interaction between the effects of the tested baseline and added dynamics (BW × AD).

4. DISCUSSION

A human-in-the-loop experiment with seven participants was performed to verify the noticeability of added dipole dynamics during control of two aircraft-representative baseline LOES dynamics with low and high control bandwidths. Adaptation of manual control dynamics, as determined from a pilot model fitted to collected measurement data, was used to verify human pilots' sensitivity to changes to the controlled dynamics.

The results obtained from an objective, cybernetic approach based on measured human control data presented in this paper seem to be in agreement with the MUAD envelope of Wood and Hodgkinson (1980). If average objective measurements that fall outside of the 95% confidence interval of the corresponding baseline condition measurements are taken to imply a noticeable change in controlled dynamics, the objective noticeability limit would be between $\zeta_z = 0.35$ and $\zeta_z = 0.50$. There, notably degraded performance (lower RMS(e)), lower control pilot gains (K_p) and reduced pilot delays (τ_p) compared to the baseline conditions are observed. As the tested added dynamics also are outside of Wood and Hodgkinson (1980)'s MUAD envelope for $\zeta_z \geq 0.35$, these results are consistent with these envelopes defined based on subjective ratings.

When comparing the experiment data obtained with the low-BW and high-BW baseline controlled dynamics, the effects of added dipole dynamics on participants' manual control dynamics and performance are found to be remarkably similar. Especially the measured variation in RMS(e) and K_p are practically identical for both tested baselines. Therefore, unexpectedly, no clear evidence was found for the expected interaction between baseline and added dynamics (Mitchell et al., 2006). This leads to the conclusion that, based on the current experiment and range of tested conditions, MUAD envelopes could be considered independent of the baseline controlled dynamics.

The experiment data presented in this paper, though already resulting in a sizable experiment, only compared the effects of varying *one* characteristic of *one* selected type of added dynamics for *two* different baseline controlled dynamics. It is not prudent to generalize the conclusions drawn from this data to other combinations of added and baseline dynamics (Wood and Hodgkinson, 1980). Future research will focus on evaluating the individual and combined effects of both baseline and added dynamics over a wider, and more representative, range of settings.

5. CONCLUSIONS

This paper verified the effects of the bandwidth of baseline controlled dynamics on the maximum unnoticeable added dynamics (MUAD) using a cybernetic approach. Pilot control parameters were identified from human-in-the-loop data collected from seven participants and provided objective and explicit insight into the effects added dipole dynamics on pilot tracking performance and control behavior for different baseline controlled dynamics settings. For the limited variation in added dynamics tested, the obtained results are highly consistent with MUAD envelopes from literature. Furthermore, observed changes in tracking error RMS, pilot gain and pilot delay with increasing magni-

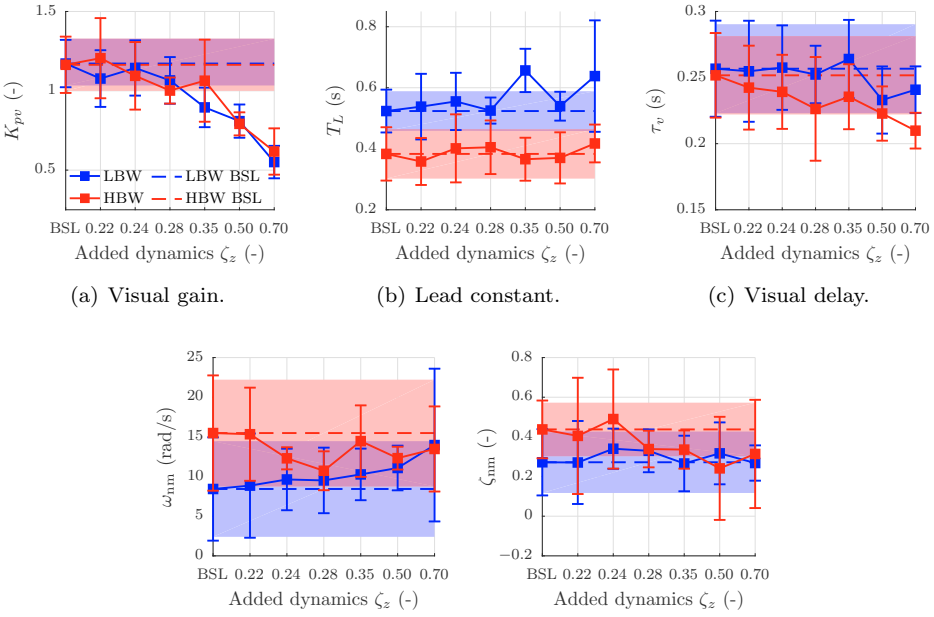

(a) Visual gain. (b) Lead constant. (c) Visual delay.

(d) Neuromuscular frequency. (e) Neuromuscular damping.

Fig. 8. Average estimated pilot model parameters, with data for the LBW baseline dynamics in blue and LBW baseline dynamics in red.

tude of the added dipole dynamics were equivalent for the compared low and high-bandwidth baseline controlled dynamics. These results suggest that, within the limited tested range of conditions, the bandwidth of the baseline controlled dynamics has no influence on the noticeability of changes in the controlled dynamics.

REFERENCES

Bosworth, J.T. and Williams-Hayes, P.S. (2007). Flight Test Results from the NF-15B Intelligent Flight Control System (IFCS) Project with Adaptation to a Simulated Stabilator Failure. In *Proceedings of the AIAA Infotech@Aerospace Conference and Exhibit, Rohnert Park (CA)*, AIAA-2007-2818.

Carpenter, C.G. and Hodgkinson, J. (1980). V/STOL Equivalent Systems Analysis. Technical Report NADC-79141-60, Naval Air Development Center.

Field, E.J., Rossitto, K.F., and Hodgkinson, J. (2003). Identification of Frequency Responses from Flight Data and Their Application for Flying Qualities Analyses. In *Proceedings of the AIAA Atmospheric Flight Mechanics Conference and Exhibit, Austin (TX)*, AIAA-2003-5537.

Geluardi, S., Nieuwenhuizen, F.M., Pollini, L., and Bülthoff, H.H. (2014). Frequency Domain Identification of a Light Helicopter in Hover. In *Proceedings of the AHS 70th Annual Forum, Montreal, Canada*.

Hodgkinson, J. (2005). History of Low-Order Equivalent Systems for Aircraft Flying Qualities. *Journal of Guidance, Control, and Dynamics*, 28(4), 577–583.

McRuer, D.T. and Jex, H.R. (1967). A Review of Quasi-Linear Pilot Models. *IEEE Transactions on Human Factors in Electronics*, HFE-8(3), 231–249.

MIL (2004). Flying Qualities of Piloted Aircraft. Technical Report MIL-STD-1797A, Department of Defence.

Mitchell, D.G., Hoh, R.H., He, C., and Strope, K. (2006). Determination of Maximum Unnoticeable Added Dynamics. In *Proceedings of the AIAA Atmospheric Flight Mechanics Conference and Exhibit, Keystone (CO)*, AIAA-2006-6492.

Mulder, M., Zaal, P.M.T., Pool, D.M., Damveld, H.J., and van Paassen, M.M. (2013). A Cybernetic Approach to Assess Simulator Fidelity: Looking back and looking forward. In *Proceedings of the AIAA Modeling and Simulation Technologies Conference, Boston (MA)*, AIAA-2013-5225.

Neal, T.P. and Smith, R.E. (1971). A Flying Qualities Criterion for the Design of Fighter Flight-Control Systems. *Journal of Aircraft*, 8(10), 803–809.

Pool, D.M. and Zaal, P.M.T. (2016). A Cybernetic Approach to Assess the Training of Manual Control Skills. In *Proceedings of the 13th IFAC/IFIP/IFORS/IEA Symposium on Analysis, Design, and Evaluation of Human-Machine Systems, Kyoto, Japan*.

van Paassen, M.M. and Mulder, M. (1998). Identification of Human Operator Control Behaviour in Multiple-Loop Tracking Tasks. In *Proceedings of the Seventh IFAC/IFIP/IFORS/IEA Symposium on Analysis, Design and Evaluation of Man-Machine Systems, Kyoto Japan*, 515–520.

Wood, J.R. and Hodgkinson, J. (1980). Definition of Acceptable Levels of Mismatch for Equivalent Systems of Augmented CTOL Aircraft. Technical Report MDC A6792, McDonnell Aircraft Company, St. Louis (MO).

Zaal, P.M.T., Pool, D.M., Chu, Q.P., van Paassen, M.M., Mulder, M., and Mulder, J.A. (2009a). Modeling Human Multimodal Perception and Control Using Genetic Maximum Likelihood Estimation. *Journal of Guidance, Control, and Dynamics*, 32(4), 1089–1099.

Zaal, P.M.T., Pool, D.M., de Bruin, J., Mulder, M., and van Paassen, M.M. (2009b). Use of Pitch and Heave Motion Cues in a Pitch Control Task. *Journal of Guidance, Control, and Dynamics*, 32(2), 366–377.